Journal of Intelligent & Robotic Systems (2023) 107:51
https://doi.org/10.1007/s10846-023-01843-0

SHORT PAPER

Divergent Component of Motion-Based Gait Intention Detection Method Using Motion Information From Single Leg

Hye-Won Oh[1] · **Young-Dae Hong**[1]

Received: 17 September 2021 / Accepted: 13 February 2023

Abstract
This paper proposes a gait intention detection (GID) method based on motion information from a single leg. This method detects three gait states: stair ascending (SA), stair descending (SD), and level walking (LW). The GID is a highly important factor for the control of gait assistive devices. If the GID is limited to the motion information from a single leg, analyzing the gait motions becomes more challenging, owing to the absence of information regarding the phase difference between both legs. To address this challenging, previous GID methods have used fusion data from several sensors. In this paper, only three inertial measurement units are used for proposed single leg GID method. To analyze gait motions using these limited sensors, the divergent component of motion (DCM) of the user is computed. The DCM is a physical quantity incorporating the linear position and linear velocity of the center of mass; these can be computed from the kinematic data of a support leg. In each of the three gait states SA, SD, and LW, the DCM shows different patterns. To classify and detect these different patterns, a pattern recognition method based on an artificial neural network algorithm is used. The GID performance of the proposed method was experimentally evaluated, and it showed 99% success rate for the SA, SD, and LW states.

Keywords Gait intention detection (GID) · Divergent component of motion (DCM) · Inertial measurement unit (IMU) · Artificial neural network · Pattern recognition

1 Introduction

Walking ability is often an important factor in determining quality of life. However, many people suffer from an impaired walking ability owing to aging or various injuries. Therefore, the development of gait assistive devices (such as robotic exoskeletons and orthoses) has received significant attention as a field of study for more than four decades. When controlling these devices, one of the most critical factors is to ensure they do not take different motions from user's intention. Therefore, a reliable gait intention detection (GID) method is required, and many corresponding studies have been performed.

Various types of data have been used for detecting gait intention. Some studies have introduced methods for manually inputting the intended walking state using a push-button interface [1–3]. These methods have the advantage of being simple to implement; however, they can lead to inconvenience for users, because they must be aware of and indicate all their gait intention. Therefore, recent studies have adopted automatic GID methods using bio-signal sensors or physical sensors. Using bio-signal sensor has the advantage of being able to quickly detect an intention of motion prior to actual movement [4–6]. However, different data can be obtained for the same gait motion owing to several factors (e.g., muscle fatigue, degree of muscle contraction, and different positions of electrode attachment [7]), and it may lead to GID failures. In contrast, physical sensors have an advantage in similar data can be obtained for the same gait motion in various situations. Therefore, to develop accurate GID methods, many studies have adopted physical sensors such as gyroscopes [8–10], force-sensitive resistors [8, 11, 12], accelerometers [13, 14], and inertial measurement units (IMUs) [11, 15–19]. Among them, some straightforward GID methods only focus on detecting gait cycle phase (e.g., stance, swing, hill strike, and toe off) [8–14]. For more precise gait assistance in daily life, some other GID methods consider various gait states, including stair ascending (SA), stair descending (SD), and level walking (LW) [15–20].

✉ Young-Dae Hong
ydhong@ajou.ac.kr

[1] Department of Electrical and Computer Engineering, Ajou University, Suwon 16499, Korea

Published online: 28 March 2023

Most of the previous methods for detecting various gait states using physical sensors typically use information of both legs. However, some people suffer from weakness or paralysis in one leg, and they only require one-leg assistive devices. In this case, detecting accurate gait states becomes more challenging, because sensor data are limited to one-leg, and the information regarding the phase difference between both legs cannot be used. To address this limitation, some studies have used fusion data from several physical sensors [17, 18, 20]. However, they require bulky or complex hardware designs for their sensor systems, which may disturb the user's natural gait motion. Furthermore, from a commercial standpoint, the higher number of used sensors, the more expensive and difficult to maintain.

In this paper, we propose a GID method using only motion information from a single leg. It can detect three gait states (SA, SD, and LW) with only three small and light IMUs, which do not affect the user's natural gait motion. In addition, this method is applicable to various forms of assistive devices, as the IMUs only need to be attached to the user's shin, thigh, and torso using Velcro fasteners (see Fig. 1). To analyze gait motions using these limited sensors, the user's 3-dimentional (3-D) divergent component of motion (DCM, also called Capture Point) [21, 22] was computed. The DCM is a physical quantity that incorporates the changes in the linear position and linear velocity for the center of mass (COM). Using this physical quantity, the gait motion can be analyzed for a three-dimensional (3-D) space with only one support leg's data. Each of three gait states (SA, SD, and LW) shows different DCM patterns. Therefore, the pattern recognition method of an artificial neural network (ANN) algorithm is used to classify and detect the current gait state.

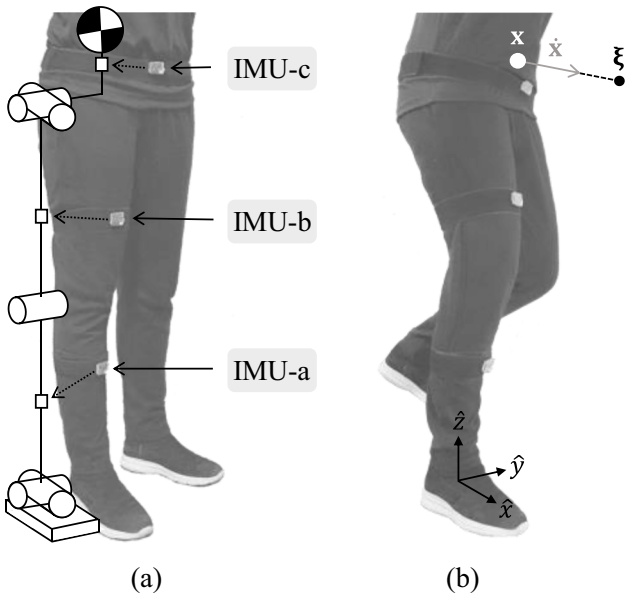

Fig. 1 **a** Appearance of user standing upright with attached IMUs and kinematic model for the proposed GID method, which has five revolute joints and DOFs. **b** Appearance of user descending the stair; and point of the DCM

The remainder of this paper is organized as follows. In Section 2, the processes for the human body DCM computation and pattern recognition via ANN training are described. In Section 3, the experimental results are discussed to evaluate the performance of the proposed GID method. In Section 4, conclusions and possible future directions are presented.

2 Gait Intention Detection Method

In this study, GID was performed during the right leg stance phase. Figure 1 shows a kinematic model for the proposed GID method, and the appearance of the user's lower body. As shown in Fig. 1(a), the COM is at the center of the lower abdomen. This model has five degrees of freedom (DOFs) with five revolute joints (the pitch joints of the ankle, knee, and hip; and roll joints of the ankle and hip). Three IMUs are attached at the front of the right shin (IMU-a), right thigh (IMU-b), and torso (IMU-c), and measure the angles and angular velocities. In this study, the pitch angles of the shin, thigh, and torso are denoted as ϕ_{aP}, ϕ_{bP}, and ϕ_{cP}, respectively, and the roll angles of the shin and torso are denoted as ϕ_{aR} and ϕ_{cR}, respectively.

The proposed GID method is divided into two parts: the DCM computation for the human body, and the pattern recognition by the ANN training. The former part is described in Section 2-1. As described in this section, the linear position and linear velocity of COM are calculated using the IMU data. Using these COM data, the time-varying DCM of the human body is computed. The latter part is explained in Section 2-2. In this part, the shallow ANN is used to train a classification model, which accurately classifies the different DCM patterns of the three gait states (LW, SA, and SD).

2.1 Calculating the Time-Varying DCM of Human Body

The DCM is the physical quantity normally used for human walking analysis [21], and walking control or motion planning for a bipedal robot [22]. It includes the linear position and linear velocity information of COM. In other words, if DCM of the user is computed during gait, the change of COM movement can be known in real time. The DCM is defined as follows [22]:

$$\boldsymbol{\xi} = \mathbf{x} + b\dot{\mathbf{x}} \tag{1}$$

where $\boldsymbol{\xi} = [\xi_x\, \xi_y\, \xi_z]^T$ is 3-D DCM, and $\mathbf{x} = [x_{com}\, y_{com}\, z_{com}]^T$ and $\dot{\mathbf{x}} = [\dot{x}_{com}\, \dot{y}_{com}\, \dot{z}_{com}]^T$ are the 3-D linear position and linear velocity of COM, respectively. As shown in Fig. 1(b), DCM is defined as a point in front at a certain distance in the direction of COM movement from current COM position. In (1), b is a time constant of DCM dynamics. It is defined as $b = \sqrt{z_{mean}/g}$, where z_{mean} is the mean value of z_{com} that is measured by a few footsteps for each of SA, SD, and LW states; and g is the gravitational acceleration.

In this study, to obtain $\mathbf{x}$ for the human body, the forward kinematics is computed from the right foot to COM. For this computation, coordinate frames (Σ_i, $i = 1, 2, \cdots, 6$) are attached as shown in Fig. 2. The base frame (Σ_0) is fixed to the right ankle during the right leg stance phase. Note that, therefore, acquired data during the right leg swing phase are not used for the proposed GID method. The joint angles $\boldsymbol{\theta} = [\theta_1\theta_2 \cdots \theta_5]$ are calculated using the orientation of the links measured via IMUs, as follows:

$$\begin{aligned} &\theta_1 = \phi_{aP}, \quad \theta_2 = \phi_{aR}, \quad \theta_3 = \phi_{bP} - \phi_{aP}, \\ &\theta_4 = \phi_{cR} - \phi_{aR}, \quad \theta_5 = \phi_{cP} - \phi_{bP}. \end{aligned} \tag{2}$$

The linear velocity of COM $\dot{\mathbf{x}}$ is computed using the Jacobian matrix. The angular velocities of each joint are acquired via IMUs in the same manner as (2). Using these processes, DCM of the user can be computed during gait.

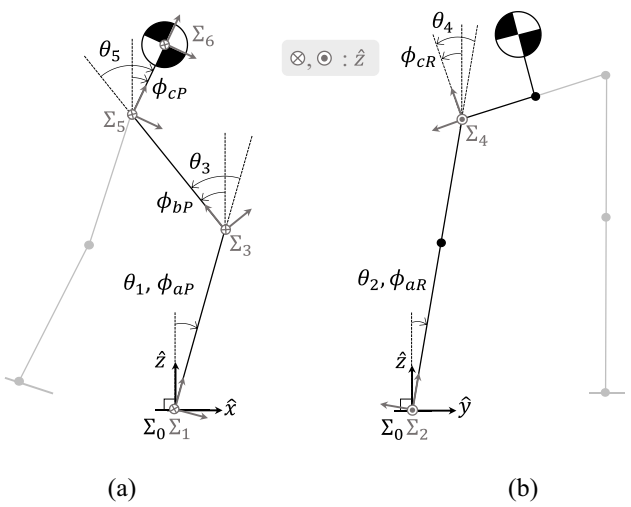

Fig. 2 Definition of coordinate frames $\Sigma_i (i = 1, 2, \cdots, 6)$ and parameters ϕ and θ in the (**a**) sagittal plane and (**b**) frontal plane. ϕ denotes link orientation measured by IMUs and θ denotes joint angle

2.2 Intention Detection by the Artificial Neural Network

An ANN is used to train a classification model that classifies the gait states SA, SD, and LW during gait. Figure 3 shows the structure of the ANN used in this study. Note that, shallow and basic ANN training with a feed-forward structure was used so that DCM could be analyzed solely on its own merits the physical quantity as the gait information for the GID method. The network has one hidden layer with twenty neurons. The sigmoid is used as the activation function of the hidden layer. In addition, as this ANN is used for multi-class classification, the soft-max is used as an activation function of the output layer.

An input layer data set is defined as $\sum_{n=0}^{k} \boldsymbol{\xi}(t - nT_s)$, where t is the current time, T_s is the sampling time of the system, and k is the total number of time series in $\boldsymbol{\xi}$ set constituting one input layer data set. The output layer includes twelve classes $C_i (i = 1, 2, \cdots, 12)$ assigned to the DCM patterns of three gait states (SA, SD, and LW) and nine exception (EXC) states. The C_1 is a SA pattern class collected when the knee is extended for SA; The C_2 is a SD pattern class collected when the knee is bent for SD; The C_3 is a LW pattern class collected when the COM moves forward over the support foot, so that the weight is loaded on the right knee. The EXC classes are determined as follows: the DCM patterns of the C_4, C_7, and C_{10} classes are collected between moments of hill-strike and toe-strike, for SA, SD, and LW, respectively; the DCM patterns of the C_5, C_8, and C_{11} classes are collected between moments of the toe-strike and just before the gait intention initiation, for SA, SD, and LW, respectively; and the DCM patterns of the C_6, C_9, and C_{12} classes are collected between the moments right after the gait intention initiation and the end moment of the right leg stance phase, for SA, SD, and LW, respectively. To train these output classes,

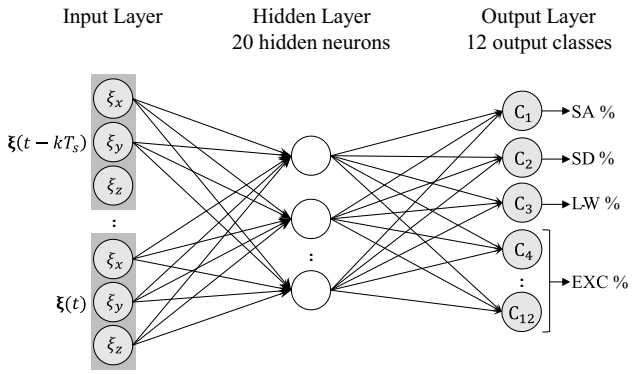

Fig. 3 Structure of the ANN classification model used for pattern recognition. An input layer data set consists of $\boldsymbol{\xi}(t)$, $\cdots$,$\boldsymbol{\xi}(t - kT_s)$, which are the time series sets. The hidden layer has twenty hidden neurons. The output layer includes twelve output classes $C_i (i = 1, 2, \cdots, 12)$ for the SA, SD, and LW states, and nine EXC states

N input layer data sets are collected for each of three gait states, and M input layer data sets are collected for each of nine EXC states. Therefore, the total number of input layer data sets used for ANN training is $3N + 9M$. To collect the input layer data sets for training the twelve output classes, the user walks $N/2$ footsteps in each gait state (SA, SD, and LW). Then, the input layer data sets for each gait state are acquired twice per one footstep with a very short time difference to improve the robustness of the trained ANN classification model.

At every gait state, the magnitudes of the fluctuations of ξ_x, ξ_y, and ξ_z are different. Therefore, ξ_x, ξ_y, and ξ_z are normalized into [0, 1], so that every data value in the input data sets can affect the ANN training. For this normalization, the maximum and minimum values of the data are required. However, because humans cannot walk at completely identical velocities, the maximum and minimum values of the DCM are not fixed, even when acquire from the same person. To address this problem, a data augmentation technique is used for the input data. Different maximum and minimum values of the DCM are used in normalization per one-third of the input layer data sets.

As the soft-max is used as an activation function of the output layer, ANN outputs probability distributions of the detected gait state classes. Therefore, to indicate the definite gait state, a state with more than 90% probability is determined as a current gait state. Also $100T_s$ delay is applied after a current gait state is determined to prevent any gait state being detected multiple times per one footstep.

3 Experimental Results

The performance of the proposed GID model was evaluated and compared with that of other GID models in which the ANN classification models were trained only using partial components of DCM. The aims of this evaluation and comparison were to verify whether the proposed method can properly detect gait intentions, and to confirm whether all components of DCM are required for accurate GID.

The DCM can be divided into several components based on three-axis information (ξ_x, ξ_y, and ξ_z), or based on the linear position and linear velocity information of the COM ($\mathbf{x}$ and $\dot{\mathbf{x}}$). By using these components alone or in combination, other GID models were trained. In this study, these GID models were trained using ξ_x only (MX), ξ_y only (MY), ξ_z only (MZ), $\mathbf{x}$ only (MP), and $\dot{\mathbf{x}}$ only (MV); and by combining ξ_x and ξ_y (MXY), ξ_x and ξ_z (MXZ), ξ_y and ξ_z (MYZ), and $\mathbf{x}$ and $\dot{\mathbf{x}}$ (MPV). The proposed GID model, which used every component of the DCM, is indicated as MXYZ. The difference between MXYZ and MPV is that MXYZ has a total of three input components: ξ_x, ξ_y, and ξ_z; in contrast, MPV has a total of six input components: x_{com}, y_{com}, z_{com}, $\dot{x}_{com}$, $\dot{y}_{com}$, and $\dot{z}_{com}$.

3.1 Experimental Setup

The experiments were conducted with one healthy female user who does not suffer any impairment of ambulatory abilities. Each sensor system for data acquisition is divided into two wireless units: the IMUs and one receiver unit. For the experiment, three IMUs were attached to the right shin, right thigh, and torso of the user, respectively. The receiver unit was connected to a microcontroller unit board for transmitting the data to a personal computer. Using the MATLAB, the computation for DCM, ANN training, and GID were carried out. The sampling time was set as 4 ms. The parameters for the ANN training, k, N, and M, were decided heuristically to 60, 60, 120, respectively to require minimal input data.

3.2 Gait Intention Detection Experimental Results

To collect the test data for evaluating the success rates, the user walked 200 footsteps per each gait states SA, SD, and LW during the right leg swing phase. The data were collected over two days to consider the diversity of the gait motions from the same person.

The GID success rates of MXYZ, MXZ, MYZ, MP, MV, and MPV are presented in Table 1. Every GID model trained with different partial component configurations was tested; however, some GID models having too low average success rates (less than 10%) are not discussed in this section. As shown in Table 1, MXYZ properly detected all three gait states with an average success rate of 99%. In contrast, the average success rates of the other GID models, in which trained with only partial components of DCM, are below 90%. In most cases, this is owing to the LW state or both the SD and LW states. From the analysis of the probability distribution of the ANN output, the most frequent cause of GID error was the classification confusion due to the similar DCM patterns of the LW and SD states. Among the GID models in Table 1, MYZ had the lowest average success rate owing to this reason.

Table 1 GID success rate. In the brackets, the numbers of GID successes for two hundred footsteps are shown. Among ANN models, the first one is the proposed method's model

ANN Model	SA [%]	SD [%]	LW [%]	Average [%]
MXYZ	99 (198)	99 (198)	99 (198)	99
MXZ	98 (196)	98 (196)	71 (142)	89
MYZ	96 (192)	46 (92)	10.5 (21)	51
MP	74.5 (149)	49 (98)	63 (126)	62
MV	90 (180)	95.5 (191)	85.5 (171)	90
MPV	96 (192)	94.5 (189)	63 (126)	85

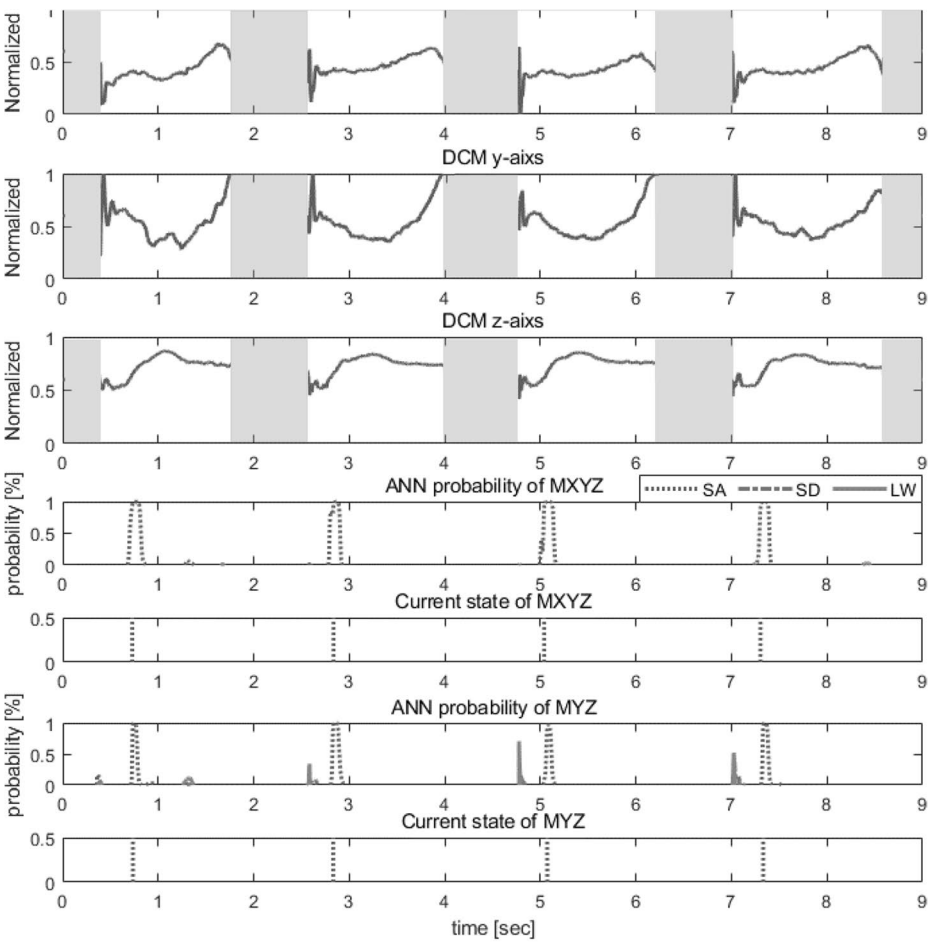

Fig. 4 The GID experimental results of SA gait motion. **a** DCM data, ANN probability results, and current state of MXYZ and MYZ. **b** Linear position and linear velocity data of the COM, ANN probability results, and current state of MPV

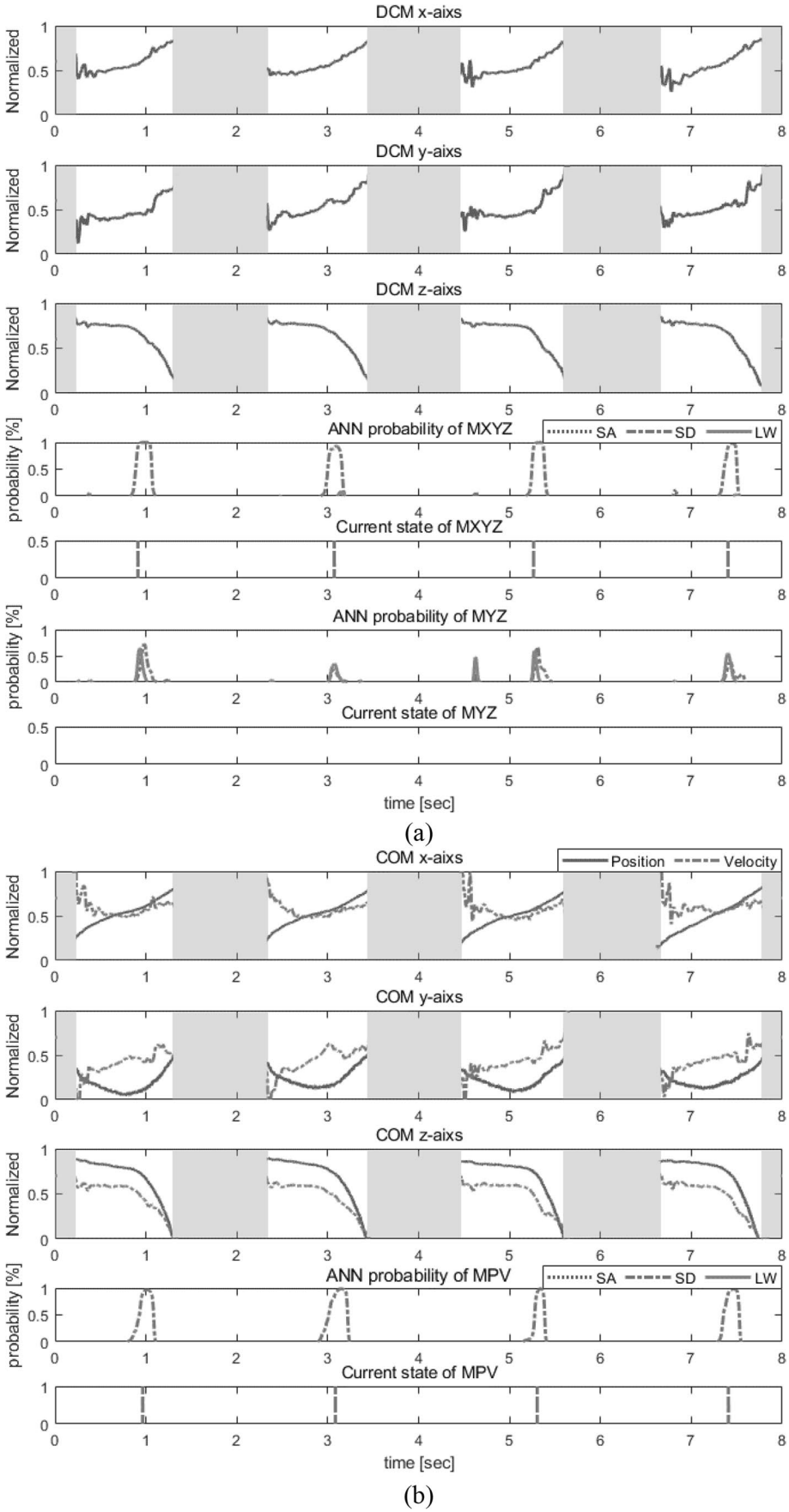

Fig. 5 The GID experimental results of SD gait motion. **a** DCM data, ANN probability results, and current state of MXYZ and MYZ. **b** Linear position and linear velocity data of the COM, ANN probability results, and current state of MPV

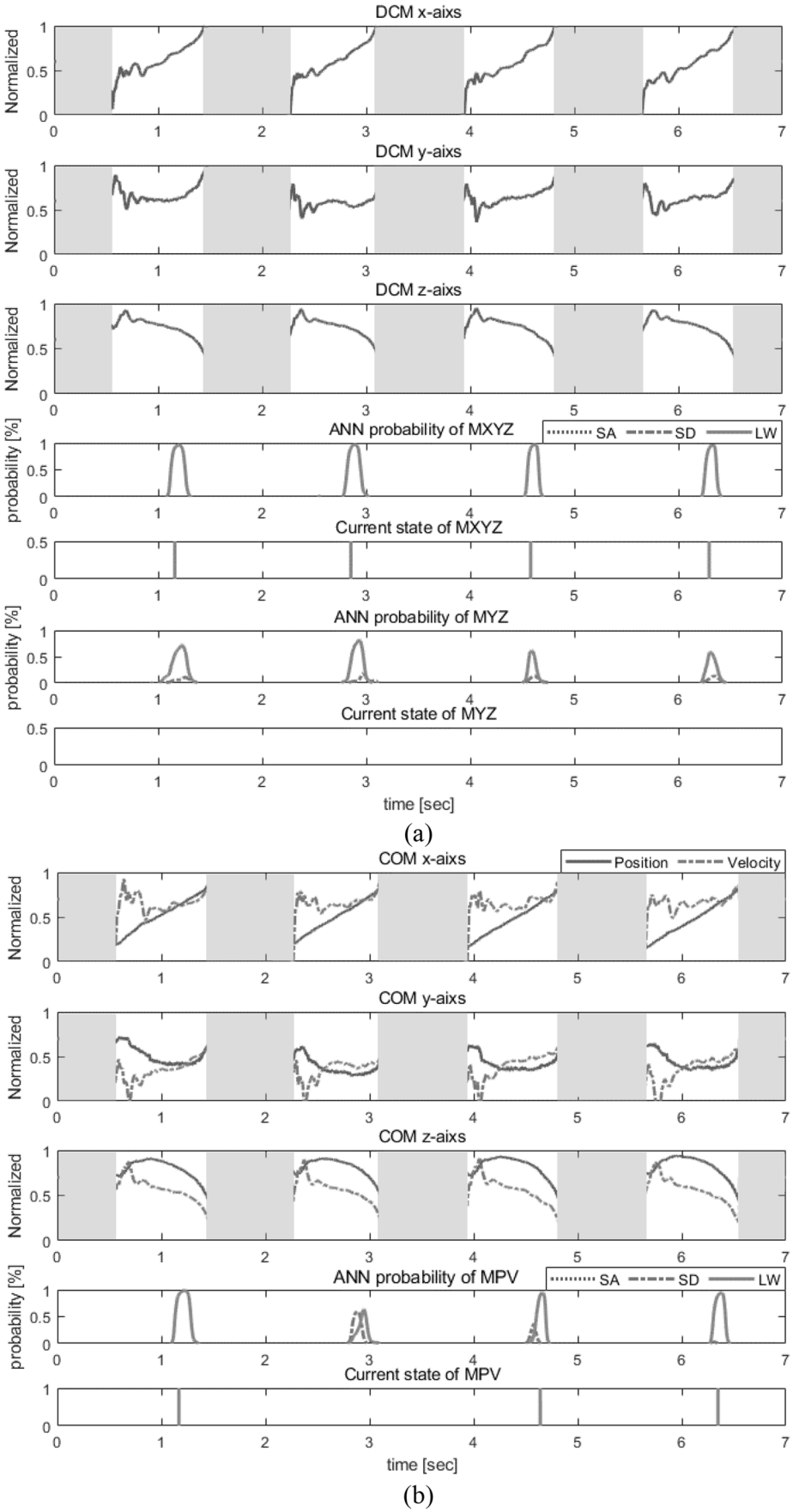

Fig. 6 The GID experimental results of LW gait motion. **a** DCM data, ANN probability results, and current state of MXYZ and MYZ. **b** Linear position and linear velocity data of the COM, ANN probability results, and current state of MPV

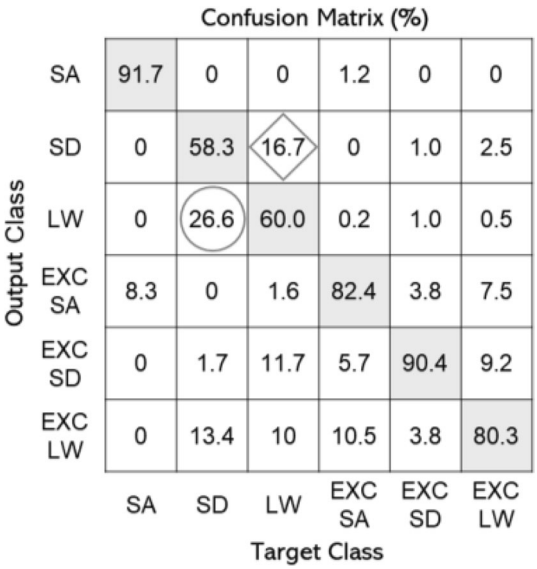

Fig. 7 Confusion matrix of MYZ. Each number in the circle and diamond indicates the error percentage of the ANN model detecting the SD state as the LW state, and detecting the LW state as the SD state, respectively

Figures 4, 5 and 6 present the GID experimental results of MXYZ, MYZ, and MPV. Note that, since the proposed GID method was only conducted during the right leg stance phase, the measured data during the right leg swing phase are not used for the method, and they do not represent the DCM either. Therefore, the acquired data during the right leg swing phase were covered with the gray box to not distract from meaningful data. The divisions for right leg stance and swing phases were measured roughly by using a switch sensor while walking. The figures show that MXYZ, the GID model of the proposed method, can successfully detect gait intentions. In each graph, the ANN probability of MXYZ increases to over 90% for the pertinent gait state at the moment the user initiates taking an intended gait state. As seen in Figs. 5 and 6, the DCM and COM linear position and velocity patterns for the SD and LW states are very similar. At the moment the user initiates gait state SD or LW; ξ_x, x_{com}, and $\dot{x}_{com}$ are increased; ξ_y, y_{com}, and $\dot{y}_{com}$ are maintained or increased; and ξ_z, z_{com}, and $\dot{z}_{com}$ are decreased. Therefore, if only some components of the DCM are used for GID, the information for distinguishing between the SD and LW states is insufficient, and the classification probabilities for both states increase simultaneously and collide. Eventually, neither state is detected as a current state (see the ANN probability and current state of MYZ in Figs. 5(a) and 6(a), and MPV in Fig. 6(b)).

The probability collision between the SD and LW states in MYZ also can be seen in the confusion matrix in Fig. 7. The confusion matrix is used to verify the performance of

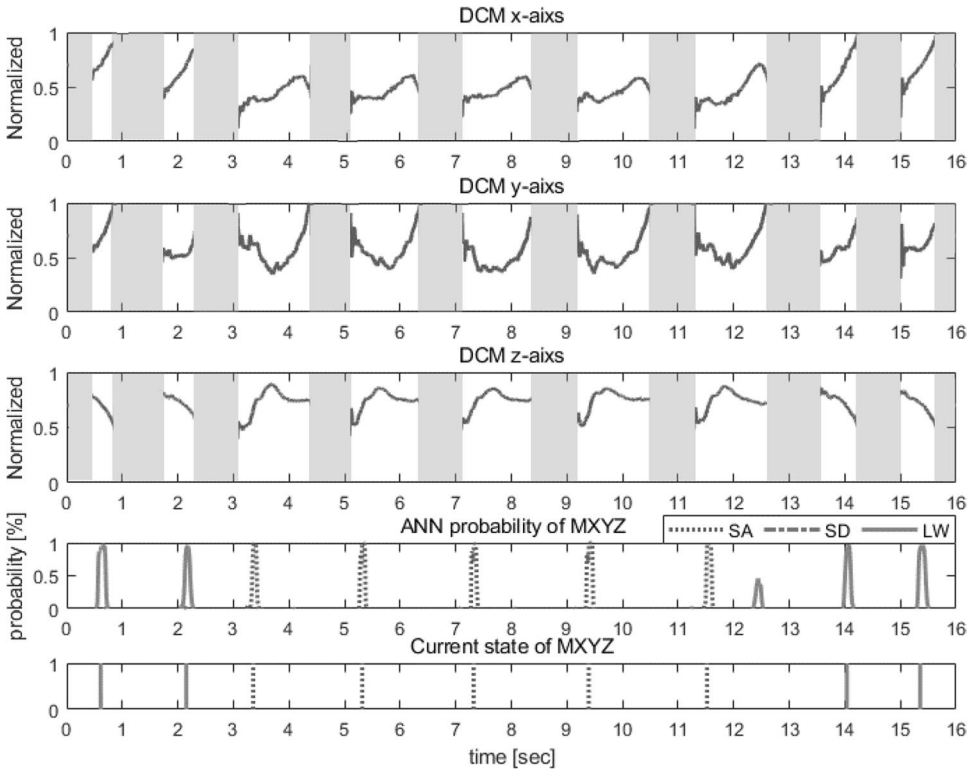

Fig. 8 GID experimental results of LW → SA → LW gait motions with different gait speed; DCM data, ANN probability results, and current state of MXYZ

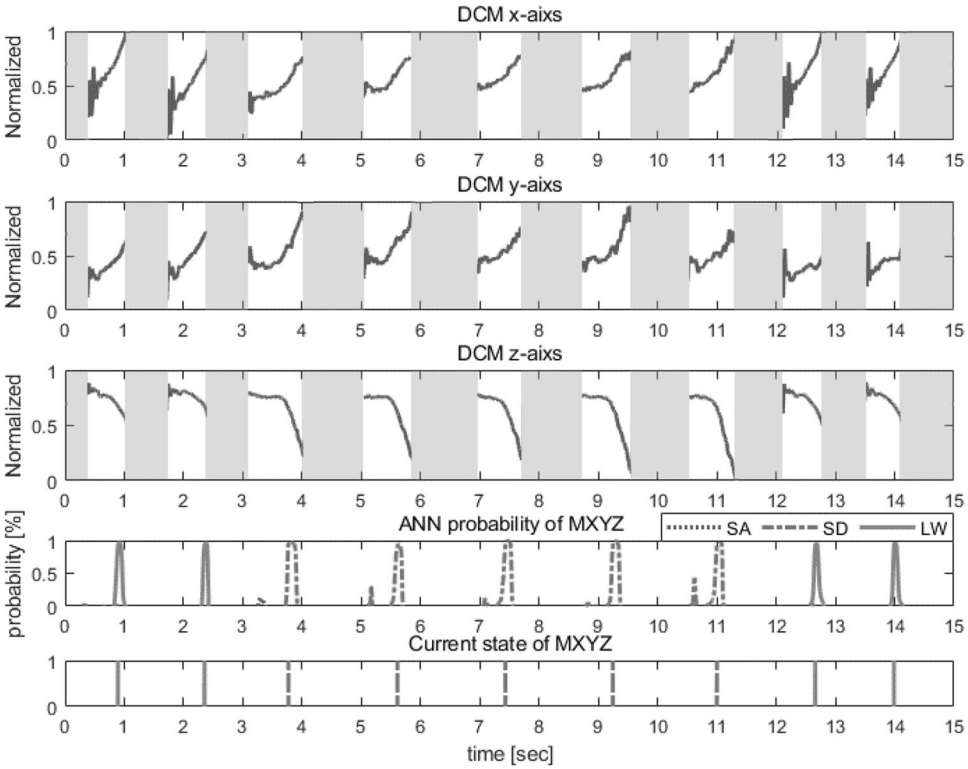

Fig. 9 GID experimental results of LW → SD → LW gait motions with different gait speed; DCM data, ANN probability results, and current state of MXYZ

a classification model. The numbers in the figure indicate the percentage of the predicted output class for each target class (nine EXC classes are grouped into three EXC classes corresponding to each gait state) during the ANN training of MYZ. The percentage for MYZ classifying the SD state as the LW state is 26.6% (in the circle), and the percentage for detecting the LW state as the SD state is 16.7% (in the diamond). These two values are the highest values among the classification errors of the SD and LW classes. Therefore, Fig. 7 shows numerically that the reason for the low GID success rate of the SD and LW classes is the collision between the two gait states. Accordingly, although each DCM component (ξ_x,ξ_y, ξ_z, $\mathbf{x}$, and $\dot{\mathbf{x}}$) contains information regarding gait motions, all components of the DCM are required to successfully classify and detect the various gait states.

Additional GID experiments were conducted in different environments to demonstrate the robustness of the proposed GID method. The experimental results are shown in Figs. 8 and 9. The user performed the GID experiments including gait state transitions between level walking and stair walking (LW → SA → LW, and LW → SD → LW) and walked with a faster gait speed than in the prior experiments (in other words, faster than when user had walked to collect the input layer data sets for the ANN training). As seen in these figures, the proposed GID method successfully detected each gait intention, even just after the gait state transition.

Consequently, the above experimental results demonstrate that the proposed GID method using DCM can detect gait intentions for several gait states (SA, SD, and LW) with high accuracy and robustness. Moreover, we verified that every component of DCM (ξ_x, ξ_y, and ξ_z) is required for successful GID using motion information from a single leg. If only partial components of DCM are used, the GID success rate decreases, owing to the similarity of the DCM patterns for the SD and LW states.

4 Conclusion

In this paper, we proposed a DCM-based GID method for detecting SA, SD, and LW states using single leg information. When the collectible information is limited from the one leg, accurate GID becomes more challenging. In this study, the challenge was addressed using DCM, which includes the linear position and linear velocity information of COM. The 3-D DCM of the user was computed during the gait using data of three IMUs attached to the right leg and torso. In each of the three gait states SA, SD, and LW, the DCM showed different patterns, and these were classified and detected via ANN training. The experimental results showed that the proposed GID method can detect each gait state (SA, SD, and LW) with 99% success rate; and every component of DCM are necessary for a more accurate GID.

In future work, we will examine the generality of the proposed method with multiple users with various heights and gait motions. Furthermore, we will conduct experiments while wearing gait assistive devices, so that the GID environment is more similar to the actual usage environment.

Authors' Contributions Hye-Won Oh conducted methodology, validation, and writing-original draft; Young-Dae Hong conduced conceptualization, methodology, and writing-review & editing.

Funding This work was supported by the National Research Foundation of Korea(NRF) grant funded by the Korea government(MSIP) (No. 2022R1C1C1002838).

Code Availability Not applicable.

Declarations

Ethics Approval Not applicable.

Consent to Participate Not applicable.

Consent for Publication Not applicable.

Conflicts of Interest/Competing Interests The authors declare no conflict of interest.

References

1. Neuhaus, P.-D. et al.: Design and evaluation of Mina: a robotic orthosis for paraplegics, in Proc. IEEE Int. Conf. Rehab. Robot. 1–8 (2011)
2. Farris, R.-J., Quintero, H.-A., Goldfarb, M.: Preliminary evaluation of a powered lower limb orthosis to aid walking in paraplegic individuals. IEEE Trans. Neural. Syst. Rehabil. Eng. **19**(6), 652–659 (2011)
3. Talaty, M., Esquenazi, A., Briceno, J. E.: Differentiating ability in users of the ReWalk ™ powered exoskeleton: an analysis of walking kinematics, in Proc. IEEE 13th Int. Conf. Rehabil. Robot. 1–5, (2013)
4. Fleischer, C., Hommel, G.: A human-exoskeleton interface utilizing electromyography. IEEE Trans. Robot. **24**(4), 872–882 (2008)
5. Sankai, Y.: HAL: Hybrid assistive limb based on cybernetics. Robot. Res. **66**, 25–34 (2010)
6. Zhang, F., et al.: Real-time implementation of an intent recognition system for artificial legs. Proc. Conf. IEEE Eng. Med. Biol. Soc. **2011**, 2997–3000 (2011)
7. Tkach, D., Huang, H., Kuiken, T.: Study of stability of time-domain features for electromyographic pattern recognition. J. Neuroeng. Rehabil. **7**(21), 1–13 (2010)
8. Pappas, I.P., et al.: A reliable gait phase detection system. IEEE Trans. Neural. Syst. Rehabil. Eng. **9**(2), 113–125 (2001)
9. Formento, P.C., et al.: Gait event detection during stair walking using a rate gyroscope. Sensors **14**(3), 5470–5485 (2014)
10. Zarika, M. et al.: Heuristic based gait event detection for human lower limb movement, in Proc. IEEE EMBS Int. Conf. Biomed. Health. Inform. 337– 340 (2017)
11. Goršič, M., et al.: Online phase detection using wearable sensors for walking with a robotic prosthesis. Sensors **14**(2), 2776–2794 (2014)
12. Agostini, V., Balestra, G., Knaflitz, M.: Segmentation and classification of gait cycles. IEEE Trans. Neural Syst. Rehabil. Eng. **22**(5), 946–952 (2014)
13. Selles, R.W., et al.: Automated estimation of initial and terminal contact timing using accelerometers; development and validation in transtibial amputees and controls. IEEE Trans. Neural Syst. Rehabil. Eng. **13**(1), 81–88 (2005)
14. Rueterbories, J., Spaich, E.G., Andersen, O.K.: Gait event detection for use in FES rehabilitation by radial and tangential foot accelerations. Med. Eng. Phys. **36**(4), 502–508 (2014)
15. Figueiredo, J., et al.: Daily locomotion recognition and prediction: a kinematic data-based machine learning approach. IEEE Access **8**, 33250–33262 (2020)
16. Lu, H., Schomaker, L. R. B., Carloni, R.: IMU-based deep neural networks for locomotor intention prediction. Proc. IEEE/RSJ Int. Conf. Intell. Robots Syst (IROS). 4134–4139 (2020)
17. Li, Y.D., Hsiao-Wecksler, E.T.: Gait mode recognition using an inertial measurement unit to control an ankle-foot orthosis during stair ascent and descent, in ASME 2012 5th Annual Dynamic Systems and Control Conf. 743–752 (2012)
18. Young, A.J., Hargrove, L.J.: A classification method for user independent intent recognition for transfemoral amputees using powered lower limb prostheses. IEEE Trans. Neural Syst. Rehabil. Eng. **24**(2), 217–225 (2016)
19. Jang, J. et al.: Preliminary study of online gait recognizer for lower limb exoskeletons, in Proc. IEEE/RSJ Int. Conf. Intell. Robots Syst (IROS). 5818–5824 (2017)
20. Moon, D.-H., Kim, D.-H. Hong, Y.-D.: Development of a single leg knee exoskeleton and sensing knee center of rotation change for intention detection. Sensors. **19**(18), 3960 (2019)
21. Hof, A.L.: The 'extrapolated center of mass' concept suggests a simple control of balance in walking. Human Movement Sci. **27**(1), 112–125 (2008)
22. Englsberger, J., Ott, C., Albu-Schaffer, A.: Three-dimensional bipedal walking control based on divergent component of motion. IEEE Trans. Robot. **31**(2), 355–368 (2015)

Hye-Won Oh received the B.S. degree in electronic engineering from Cheongju University, Cheongju, Korea in 2020. She is currently working toward the Ph.D. degree in electrical and computer engineering from Ajou University, Suwon, Korea. Her current research interests include exoskeleton for walking and power assist, especially in human motion intention prediction and sensor fusion for motion intention prediction.

Young-Dae Hong received the B.S., M.S., and Ph.D. degrees in electrical engineering from the Korea Advanced Institute of Science and Technology (KAIST), Daejeon, Korea, in 2007, 2009, and 2013, respectively.

Since 2014, he has been with the Department of Electrical and Computer Engineering, Ajou University, Suwon, Korea, where he is currently an Associate Professor. His current research interests include bipedal robot and exoskeleton for walking and power assist, especially in bipedal walking pattern generation and control, real-time footstep planning, human motion intention prediction, sensor fusion for motion intention prediction, and optimization-based robot control.